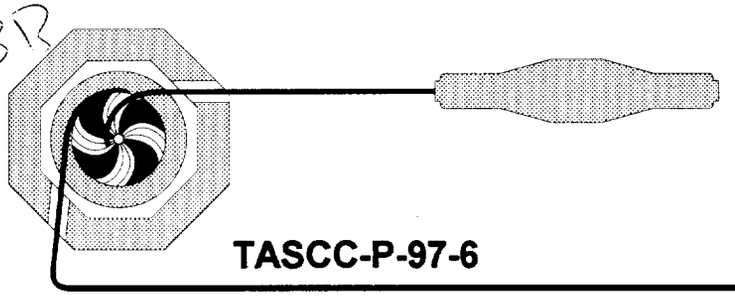

PREPRINT

tascc

TASCC-P-97-6

MEASUREMENT OF THE ℓ-FORBIDDEN GAMOW-TELLER BRANCH OF ^{37}K

E. Hagberg[1], I.S. Towner[1], T.K. Alexander[1], G.C. Ball[1], J.S. Forster[1], J.C. Hardy[1], J.G. Hykawy[1], V.T. Koslowsky[1], J.R. Leslie[2], H.-B. Mak[2], I. Neeson[2] and G. Savard[1]

[1] AECL, Chalk River Laboratories, Chalk River, Ontario K0J 1J0, Canada
[2] Department of Physics, Queen's University, Kingston, Ontario, K7L 3N6, Canada

Submitted to
Phys. Rev. C

Physical and Environmental Sciences
Chalk River Laboratories
Chalk River, ON K0J 1J0 Canada

1997 February

Measurement of the ℓ-forbidden Gamow-Teller Branch of ^{37}K

E. Hagberg[1], I.S. Towner[1], T.K. Alexander[1], G.C. Ball[1], J.S. Forster[1], J.C. Hardy[1], J.G. Hykawy[1], V.T. Koslowsky[1], J.R. Leslie[2], H.-B. Mak[2], I. Neeson[2] and G. Savard[1]

[1] *AECL, Chalk River Laboratories, Chalk River, Ontario, Canada K0J 1J0*

[2] *Department of Physics, Queen's University, Kingston, Ontario, Canada K7L 3N6*

(February 20, 1997)

Abstract

The beta decay of ^{37}K is studied in detail. Several new beta decay branches and γ-ray transitions are assigned to this nucleus. The ℓ-forbidden $0d_{3/2} \rightarrow 1s_{1/2}$ Gamow-Teller branch to the first excited state in ^{37}Ar is observed for the first time and its branching ratio measured to be $(42.2 \pm 7.5) \times 10^{-6}$. Such ℓ-forbidden branches are very sensitive to extra-nucleonic effects such as meson-exchange currents and Δ-isobar excitations. A calculation of these as well as core-polarization and relativistic effects, predict branching ratios of 8×10^{-6} with USD wavefunctions and 52×10^{-6} with Chung-Wildenthal wavefunctions.

21.10.-k,21.60.Cs,23.40.-s,27.30.+t

I. INTRODUCTION

Studies of ℓ-forbidden Gamow-Teller and isovector M1 transitions are a sensitive probe of the possible influence of extra-nucleonic effects, such as meson-exchange currents or Δ-isobar excitations, on the description of low-lying nuclear states. These transitions are special, in that ordinary nuclear effects produce only very small transition matrix elements and extra-nucleonic effects thus become more visible. In the case studied here, M1 transitions between $3/2^+$ and $1/2^+$ states, the matrix element would be identically zero in the long wavelength approximation if it were assumed the decay proceeds entirely through a single-particle $d_{3/2}$ to $s_{1/2}$ transition. Of course, in practice a transition is never exactly single particle in nature: there will always be configuration admixtures and they must be estimated. Also, there will be corrections to the impulse approximation arising from relativistic effects. But if these two complications can be reliably evaluated, then the study of ℓ-forbidden transitions will lead directly to information on meson-exchange currents and Δ-excitations.

Comparisons of isovector M1 γ-transitions and their analogous Gamow-Teller (GT) β-transitions provide a further powerful simplification. Because of the similarities in the operators, the ratio of these matrix elements is very insensitive to the particulars of the model. Both M1 and GT matrix elements increase (or decrease) together with the choice of parameters, with their ratio remaining unchanged.

Studies of ℓ-forbidden transitions in nuclei that consist of a particle (or hole) in an LS closed shell are particularly promising because the lowest-order wavefunctions are simple and configuration admixtures can be calculated with some degree of confidence. They offer the best opportunity to study extra-nucleonic effects with minimum sensitivity to unknown details in the wavefunctions.

The ℓ-forbidden transitions in A=39 nuclides have been the subject of many studies [1–4] since they meet these criteria. The predicted GT matrix element [1,5,6], $M(GT) \equiv [B(GT; 3/2^+ \rightarrow 1/2^+]^{1/2} = -0.036(18)$, is in fair agreement with experiment [1,2], $-0.024(1)$, whereas the predicted isovector (IV) matrix element [1,5,6], $M^{(1)} \equiv [B(M1: IV, 3/2^+ \rightarrow 1/2^+]^{1/2} = -0.022(19)$, differs from experiment, $-0.091(8)$, by a factor of four. No agreement seems possible for the insensitive $M(GT)/M^{(1)}$ ratio as any reasonable adjustment in the theory of effective operators [5] has so far been unable to explain such a big discrepancy.

The tantalizing promise offered by the study of ℓ-forbidden transitions has not been fulfilled for the A=39 nuclides. The only way to obtain a further understanding of this problem is to study additional cases. The A=37 nuclei offer the next best choice in terms of nuclear-structure simplicity. Although not as simple as the A=39 cases their wavefunctions can still be calculated with confidence.

The A=37 mirror nuclides have not been studied with the same detail as the A=39 ones. The lifetime of the $1/2^+ \rightarrow 3/2^+$ M1 transition in ^{37}Ar is known [7], but that in ^{37}K is not. The ℓ-forbidden GT branch from ^{37}K also is not known. In this paper we describe the first measurement of this branch and a comparison with the calculated value from the Towner-Khanna model [5,6].

II. EXPERIMENTAL TECHNIQUE

The ^{37}K activity was produced with the ^{40}Ca(p,α) reaction. A $3\mu A$, 15 MeV proton beam from the TASCC facility bombarded a stack of fifteen 0.5 mg/cm^2 thick Ca targets inside a helium-filled target chamber. A He-jet transport system with NaCl aerosol removed the activity from the target chamber and brought it into a low background counting area. There, radioactive samples were collected on the 25 mm wide aluminized mylar tape of a fast tape transport system. Every 3.5 seconds the tape moved and the samples were sequentially positioned in front of two separate counting stations. While sample n was collecting, sample $n-1$ was counted in station 1 and sample $n-2$ was counted in station 2. Fig. 1 shows a layout of the experimental arrangement.

The sample preparation, transport and counting procedures were very similar to those used in a published experiment on the ℓ-forbidden decay of ^{39}Ca [1] and are described in detail in that report. Briefly, the first counting station consisted of a 68% efficient HPGe detector and two plastic scintillators. Its purpose was to observe γ rays originating from weak β branches of ^{37}K populating excited states in ^{37}Ar. (The ground-state transition accounts for 98% of the decay intensity.) Events observed in the HPGe detector were tagged by the coincident positrons seen in the scintillators, either heading away from the HPGe (upper scintillator) or towards the HPGe (lower scintillator). In the present experiment, the majority of events observed in the HPGe detector originated from positrons heading towards that detector because they could interact with it directly or through bremsstrahlung and annihilation-in-flight processes. Such unwanted events were removed by a condition that HPGe events must be coincident with positrons heading away from that detector. This condition lead to a dramatic reduction of the background produced by positrons from the dominant, superallowed ground-state branch, which is not accompanied by γ rays. Events from excited-state branches, which are accompanied by subsequent γ rays, are still efficiently recorded.

The second counting station was designed to measure the total ^{37}K activity of each sample. A continuous-flow gas proportional counter, with nearly 100% efficiency for positrons, was used for this purpose. The samples on the transport tape were positioned in the center of the counter and decay positrons were detected and multi-scaled.

The efficiency of the HPGe detector was determined with standard sources of ^{54}Mn, ^{56}Co, ^{60}Co, ^{88}Y, ^{137}Cs and ^{228}Th. The efficiencies of the plastic scintillators were determined by comparisons of the intensities of strong γ-ray peaks in the singles HPGe counter spectrum with the intensities of the same γ-ray peaks in the scintillator-coincident HPGe spectra. The gas counter efficiency has been determined in several previous experiments.

III. EXPERIMENTAL RESULTS

Three beta-decay branches, producing a total of four γ-ray transitions, have been previously reported for ^{37}K [7]. Our scintillator-gated γ-ray spectrum, obtained from 48,000 radioactive samples is shown in Fig. 2. It is dominated by γ rays from ^{37}K although the strongest excited-state β-decay branch from this isotope has an intensity of only 2%. Gamma rays from small quantities of ^{42m}Sc and ^{44}Sc (produced from the ^{42,44}Ca isotopes present in the natural Ca target) and ^{32}Cl, ^{52m}Mn and ^{58}Cu (produced from minute S, Cr

and Ni target contaminations, partially originating from the target fabrication process) are also visible in Figs. 2 and 3. They were used for the HPGe energy calibration. Our γ-ray spectrum contains many new peaks that we assign to the decay of ^{37}K. Fig. 3 shows two expanded areas of the γ-ray spectrum shown in Fig. 2. They display in more detail the main γ-ray peaks used to deduce the ℓ-forbidden beta-decay branch (Fig. 3a) and two weak γ rays assigned to ^{37}K that are barely visible in Fig. 2 (Fig. 3b).

Our results for the ten γ-ray transitions we assign to ^{37}K are shown in Table I. Two γ rays previously attributed to ^{37}K [8] were not observed in our experiment. Two of the ten γ rays observed were known before, the remainder are new assignments. Our assignment of the eight new γ-ray transitions to ^{37}K is based on two observations. The measured half-life of each of them agrees with the accepted value, 1.226 (7) s and their energies all agree with known level differences in the beta-decay daughter, ^{37}Ar [7].

We obtained the absolute γ-ray intensities, shown in Table I, by normalizing the HPGe data to the absolute ^{37}K decay intensity obtained from the gas counter measurements. The multi-scaled positron data from this counter were analyzed for the ^{37}K content. Excellent fits to the decay curves were obtained with two components with the half-life of the first component fixed to that of ^{37}K and the second one being a constant background. The second component accounts for activities such as ^{42m,44}Sc whose half-lives are much longer than the 3-second measurement interval and thus appear constant in our data. The number of ^{37}K decays determined from the decay-curve analysis was corrected for the detector efficiency and the decay losses experienced by the samples during the 3.5 second time spent between counting at the HPGe location and at the gas counter position. The half-life used to fit the decay curves and to calculate the decay losses was the accepted value of 1.226(7) s [7]. After a small correction for electron-capture decays (which are invisible to the gas counter) we deduce that a total of $8.58(25) \times 10^{10}$ ^{37}K decays took place at the HPGe counting location during the experiment.

We have constructed the decay scheme shown in Fig. 4 by assigning the γ rays listed in Table I to the corresponding known level energy differences in ^{37}Ar and using the absolute intensities shown in the table. This decay scheme contains five weak beta transitions that have not been observed before. Our results for all beta transitions from ^{37}K are shown in Table II. Some details for transitions of particular interest and for cases in which our data do not support previous results are discussed below.

1410 keV state, $1/2^+$. The $d_{3/2} \rightarrow s_{1/2}$ beta transition is ℓ-forbidden as is indicated by the large ft value of 7.39. The 1410 keV state de-excites by a single γ-ray transition of the same energy. It is populated, in addition to the beta feeding, by a 1386 keV γ ray and two much weaker γ rays of 2192 and 2528 keV (the latter will be discussed with the 3938 keV state). Fig. 3a shows the spectrum near the 1386 and 1410 keV γ-ray peaks. The beta branching ratio for the ℓ-forbidden transition was deduced to be 42.2(75) ppm. It will be compared to a theoretical calculation in Sec. IV.

1611 keV state, $7/2^-$. This state is populated and de-excited by γ rays of almost equal intensities. Consequently the deduced β side feeding is poorly determined, 25 ± 20 ppm, and could well be non-existent. The beta-decay branch can, within its large uncertainty range, accommodate log ft values of 8 or greater, appropriate for a unique second-forbidden transition.

2490 and 3938 keV states. We observe only one de-populating γ ray from each of these

levels. Previous in-beam γ-ray experiments have shown evidence for a second, weaker de-populating γ ray in both cases. Our data does not contradict the in-beam observations since those additional weak γ rays would be below our sensitivity limit. We have used the published γ-ray branching ratios [9], together with our measured intensity for the strong γ-ray branch, to deduce the intensities of the 879 and 2528 keV γ rays shown in Fig. 4, which were not visible in our experiment.

2796 keV state, $5/2^+$. We observe three γ-ray transitions de-populating this state. The 1185 and 1386 keV γ rays have not been reported before. We do not observe a 2217 keV γ ray, previously reported by Taras *et al.* [10] from ^{37}Cl$(p,n)^{37}$Ar studies, nor the 579 keV γ ray supposedly populating the 2217 keV level. Both should clearly have been visible to us, if present with the gamma branching ratios reported in Ref. [10]. Our deduced β-decay branch to the 2796 keV level is 2.07(11)%, which agrees with two previous results, 2.22(21)% [11] and 2.0(4)% [12], but not a third one 1.45(16)% [13].

In Table III we present the gamma branching ratios we deduce for the 2796 and 3602 keV states in ^{37}Ar. For both cases our data are superior to those in the literature [9] and for the 2796 keV case they also disagree with the literature values.

IV. THEORY AND COMPARISONS

A. The ℓ-allowed branches

The starting wavefunctions for a discussion of the nuclear spectroscopy of the A=37 nuclides are the configurations $(s,d)^{-3}$, three holes in the closed $1s$-$0d$ shells. Mixing among these configurations is calculated in the shell model with the residual interaction taken from the universal s-d (USD) interaction constructed by Wildenthal [14]. This interaction has been constrained to give good fits to the energy eigenvalues of many low-lying states in s,d-shell nuclei. For spectroscopy studies, it is the most accurate interaction available for these nuclei. For comparison purposes, we also consider the older Chung-Wildenthal (CW) interaction [15]. Brown has recently noted [16] that while the USD wavefunctions reproduce well the Gamow-Teller matrix elements for low-lying states, the CW interaction seems to do better at describing the Gamow-Teller giant resonance and its energy distribution.

Since the model space, $(s,d)^{-3}$, is a truncation of the full Hilbert space, some consideration has to be given to the renormalization of transition operators used in truncated spaces. For electromagnetic M1 and Gamow-Teller β-decay transitions, we write these operators as

$$\begin{aligned} M1 &= \left(\frac{3}{4\pi}\right)^{1/2} \{g_{\rm L,eff}\mathbf{L} + g_{\rm S,eff}\mathbf{S} + g_{\rm P,eff}[Y_2,\mathbf{S}]\}\,, \\ GT &= g_{\rm LA,eff}\mathbf{L} + g_{\rm A,eff}\boldsymbol{\sigma} + g_{\rm PA,eff}[Y_2,\boldsymbol{\sigma}], \end{aligned} \tag{1}$$

where $g_{\rm L,eff} = g_{\rm L} + \delta g_{\rm L}$ etc. with $g_{\rm L}$ the bare, impulse-approximation coupling constant and $\delta g_{\rm L}$ the correction to it. There is a new term $[Y_2,\mathbf{S}]$, absent from the bare M1 operator, which has the form of a spherical harmonic of rank 2 coupled to the spin operator to form a tensor of multipolarity 1. Likewise for the GT operator, both the $\mathbf{L}$ and $[Y_2,\boldsymbol{\sigma}]$ terms are absent from the bare operator but appear through the renormalization. Brown and Wildenthal in a series of papers [17–19] have determined the effective coupling constants, δg, for M1 and

GT operators by fitting calculations of transition rates based on the USD wavefunctions to experimental data for a large number of nuclides in the s,d shell.

An alternative to data fitting is to evaluate the coupling constants, δg, from first principles. This is practicable for nuclei described as closed-shells-plus-or-minus-one-nucleon as has been demonstrated by the work of the Chalk River and Tokyo groups [5,20,21]. There are two principal contributions to the renormalization. First, the truncated model space is corrected by inclusion of configurations from other shells via second-order perturbation theory. These corrections are called core polarization. Second, the bare operators themselves are influenced by the fact that nucleons in a nucleus are interacting by the exchange of mesons, leading to corrections known as meson-exchange currents. For GT transitions, the most important of these processes involves exciting a nucleon to its internal isobar state, the Δ resonance. Results from the calculations of Towner [5] for M1 and GT operators are compared with the fitted values of Brown and Wildenthal [17–19] in Table IV. For ℓ-allowed M1 and GT transitions, the calculations are dominated by the isovector $g_{\rm S}$ and $g_{\rm A}$ values respectively, for which there is reasonable accord between the δg values of Towner (T) and Brown-Wildenthal (BW). For ℓ-forbidden transitions between $d_{3/2}$ and $s_{1/2}$ states, only the $g_{\rm P}$ terms contribute and here there are significant differences between the calculated values of T and the fitted values of BW, particularly for the isovector M1 transitions. The study of ℓ-forbidden transitions, therefore, is aimed at shedding some light on this difference.

In the beta decay of ^{37}K reported here, six Gamow-Teller transitions have been identified, five of which are denoted ℓ-allowed and the sixth, being a $3/2^+ \rightarrow 1/2^+$ transition, is called ℓ-forbidden. The $B(GT)$ values for these transitions are listed in Table V, where it is seen that the ℓ-forbidden value is very small indicating the hindered nature of the transition. The $B(GT)$ value is related to the ft value via

$$ft = \frac{6144.6}{B(F) + B(GT)}, \tag{2}$$

where $B(F)$ is the Fermi matrix element squared and has the value unity for the isobaric analogue ground-state transition and is zero for the others. Table V also gives the calculated values using USD or CW wavefunctions and effective operators from T or BW. We note the USD wavefunctions reproduce the experimental data for the ℓ-allowed transitions better on average than the CW wavefunctions, but are noticeably inferior for the ℓ-forbidden branch.

B. The ℓ-forbidden branches

In the corresponding work in the A=39 nuclides [1–4], the $3/2^+ \rightarrow 1/2^+$ transitions are uniquely given by a single-particle $d_{3/2} \rightarrow s_{1/2}$ matrix element, and hence are uniquely related to the renormalized coupling constant, $g_{\rm P}$. In the A=37 case, configuration mixing among the $(s,d)^{-3}$ states implies the $3/2^+ \rightarrow 1/2^+$ transition involves a mix of ℓ-allowed and ℓ-forbidden matrix elements, even though up to now we have been calling this an ℓ-forbidden transition. With the USD wavefunctions, the $3/2^+ \rightarrow 1/2^+$ transition matrix element, $M(GT) \equiv [B(GT)]^{1/2}$ is

$$\begin{aligned} M(GT) = &-0.0071\langle d_5 \parallel GT \parallel d_5\rangle - 0.0091\langle d_5 \parallel GT \parallel d_3\rangle + 0.0169\langle s_1 \parallel GT \parallel s_1\rangle \\ &+0.0094\langle d_3 \parallel GT \parallel d_5\rangle + 0.2088\langle d_3 \parallel GT \parallel d_3\rangle \end{aligned}$$

$$-0.0599\langle s_1 \parallel GT \parallel d_3\rangle + 0.4549\langle d_3 \parallel GT \parallel s_1\rangle, \tag{3}$$

where the double-barred matrix elements are single-particle reduced matrix elements of the operator, Eq. (1), in the Brink and Satchler [22] conventions. In terms of effective coupling constants, the matrix element becomes

$$\begin{aligned} M(GT) &= 0.0029 g_{\mathrm{A,eff}}(s\text{-}s) - 0.0013 g_{\mathrm{A,eff}}(d\text{-}d) + 0.3895 g_{\mathrm{LA,eff}}(d\text{-}d) \\ &\quad -0.1179 g_{\mathrm{PA,eff}}(d\text{-}s) - 0.0812 g_{\mathrm{PA,eff}}(d\text{-}d), \\ &= 0.0121 g_{\mathrm{A,eff}}(d\text{-}d) - 0.1179 g_{\mathrm{PA,eff}}(d\text{-}s), \end{aligned} \tag{4}$$

where in the last line the Towner values from Table IV are used to relate $g_{\mathrm{A,eff}}(s\text{-}s)$, $g_{\mathrm{LA,eff}}(d\text{-}d)$ and $g_{\mathrm{PA,eff}}(d\text{-}d)$ to $g_{\mathrm{A,eff}}(d\text{-}d)$. Since $g_{\mathrm{A,eff}}(d\text{-}d) \sim 1.0$ and $g_{\mathrm{PA,eff}}(d\text{-}s) \sim 0.1$, one sees from Eq. (4) that the ℓ-allowed and ℓ-forbidden matrix elements are making a roughly equal contribution to $M(GT)$. This is still a sizeable ℓ-forbidden contribution compared to a typical ℓ-allowed $3/2^+ \rightarrow 3/2^+$ transition. However, because of the relative minus sign in Eq. (4) these two contributions nearly cancel each other. Therefore this transition is more sensitive to the choice of s-d shell wavefunctions, USD versus CW, than it is to the effective operators. This can be seen from Table V where there is an order of magnitude difference between the $B(GT; 3/2^+ \rightarrow 1/2^+)$ value calculated with USD and CW wavefunctions. With Towner's effective coupling constants, the branching ratio for the ℓ-forbidden transition is given by 8 ppm with USD and by 52 ppm with CW wavefunctions compared with an experimental value of 42.2(7.5) ppm.

C. The $M(GT)/M^{(1)}$ ratios

In the calculations of effective operators, the dominant contribution to the ℓ-forbidden coupling constant, $g_{\mathrm{PA,eff}}$, comes from isobar excitations. (See Table 5 of Ref. [4]). Similarly for the isovector M1 coupling constant, $g_{\mathrm{P,eff}}$, the largest contribution comes from isobars although there are sizeable contributions from other meson-exchange processs and from orbital contributions to the core-polarization calculation. To the extent that $g_{\mathrm{PA,eff}}$ and isovector $g_{\mathrm{P,eff}}$ are given entirely by isobar contributions (and spin contributions to the core-polarization calculation) these coupling constants and hence their ℓ-forbidden matrix elements will scale with each other according to the bare g_{A} and isovector g_{S} values. That is $M^{(1)} \equiv [B(M1; IV; 3/2^+ \rightarrow 1/2^+)]^{1/2}$ and $M(GT)$ are approximately in the ratio

$$\frac{M(GT)}{M^{(1)}} \simeq \frac{1.26}{4.706} \times 2 \left(\frac{4\pi}{3}\right)^{1/2} \simeq 1.1. \tag{5}$$

The puzzle is that the experimental value for this ratio, 0.26, in the A=39 nuclides [1–4] is a factor of four smaller than this estimate, while the more complete theory calculation moves the estimate upwards. It is therefore of interest to examine this ratio for the ℓ-forbidden transition in the A=37 nuclei, although to date there are less electromagnetic data available.

In ^{37}Ar, the lifetime of the $1/2^+$ state is known to be $\tau = 950(200)$ fs [7] corresponding to a width of $\Gamma = 0.69(15)$ meV. This width is made up of an M1 and an E2 component. If we use the shell model to calculate the E2 component of $\Gamma(E2) = 0.23$ meV with USD

wavefunctions and effective charges of Alexander *et al.* [23] then the M1 width is $\Gamma(M1) = 0.46(15)$ meV corresponding to an M1 matrix element $M(M1;\ ^{37}\mathrm{Ar};\ 3/2^+ \rightarrow 1/2^+) = -8.4(14) \times 10^{-2}\ \mu_N$ assuming the shell-model sign. For ^{37}K, there is only a limit on the lifetime of the $1/2^+$ state available, < 1.5 ps, corresponding to $\Gamma > 0.44$ meV. Again using the shell model to compute the E2 component, we obtain a limit on the M1 matrix element $M(M1;\ ^{37}\mathrm{K};\ 3/2^+ \rightarrow 1/2^+) > 6.8 \times 10^{-2}\ \mu_N$. The isovector combination of these matrix elements is $M^{(1)} = \frac{1}{2}(M(^{37}\mathrm{Ar}) - M(^{37}\mathrm{K}))$ and the experimental limit on the ratio $M(GT)/M^{(1)} < 0.2$. Again the experimental data point to a value of this ratio much less than the simple estimate given in Eq. (5). However, as the calculations recorded in Table VI indicate, the theory here also supports smaller values. Thus for ℓ-forbidden transitions in the A=37 nuclides there is no conflict between theory and experiment. Nevertheless, the corresponding situation in the A=39 nuclides still remains a puzzle.

D. The first-forbidden branches

First-forbidden β-decay branches are another example of hindered β transitions that have an enhanced sensitivity to extra-nucleonic effects [24,25]. In these cases, meson-exchange contributions lead to a very large enhancement of the time-component axial-charge matrix element over that expected from the impulse approximation. This enhancement occurs in rank-0 transition operators evident in first-forbidden β decay between states of the same spin and opposite parity. Warburton *et al.* [25] have, among other cases, calculated the β-decay rates for the $3/2^+ \rightarrow 3/2^-$ transitions in ^{37}K and ^{39}Ca via the impulse approximation in the nuclear shell model. The transitions in question, not known at the time of the calculation, can now be compared to measured values.

Our result for the $^{37}\mathrm{K}(3/2^+, \mathrm{gs}) \rightarrow ^{37}\mathrm{Ar}(3/2^-, 2490\ \mathrm{keV})$ β-decay branch is shown in Table VII and compared to the predicted value. Our limit for the $^{39}\mathrm{Ca}(3/2^+, \mathrm{gs}) \rightarrow ^{39}\mathrm{K}(3/2^-, 3019$ keV) branch, taken from Ref. [1], is also shown. For both cases the predicted branching ratio is about an order of magnitude larger than the measured one. This is a very strong hint that the accuracy of the shell-model calculation is insufficient for the expected enhancement of the axial-charge matrix element to be extracted from these first-forbidden decays.

E. The ft value of the ground-state branch

The ^{37}K nucleus has been chosen as a good case for precision tests of weak interaction symmetries in β decay with optically trapped sources [26]. The focus in those studies will be the superallowed, ground-state β-decay branch and its ft value needs to be precisely known. Thus, corrections need to be made for the presence of other, sizeable allowed GT branches, such as the β branch to the 2796 keV state. Our result for this branching ratio, 2.07(11)%, is the most precise one obtained so far. Our data also show that all other ^{37}K beta-decay branches, excluding those to the ground and 2796 keV states, are smaller than 250 ppm. Our experiment was designed to be sensitive to very weak β transitions. We have performed another experiment on ^{37}K, designed to measure even more precisely the β-decay branch to the 2796 keV state and the analysis of this experiment is in progress [27].

V. CONCLUSIONS

The weak β-decay branches from ^{37}K have been investigated and the strength of the ℓ-forbidden GT branch measured to be 42.2(7.5) ppm. The theoretical prediction for this branching ratio is very sensitive to the choice of s,d-shell wavefunctions used. With the effective coupling constants explicitly evaluated from core-polarization and meson-exchange processes, the branch is calculated to be 8 ppm with USD wavefunctions and 52 ppm with CW wavefunctions.

The ratio of the ℓ-forbidden GT matrix element to that of the isovector M1 matrix element is expected to be less sensitive to the details of the effective coupling-constant calculation and with some overly simplistic assumptions, it has a value of 1.1. A more detailed calculation reduces this ratio to the vicinity of 0.2 for the A=37 case, but again is sensitive to the wavefunctions chosen. By contrast, in the A=39 case, the detailed calculation increases the ratio to 1.63. The experimental situation does not follow this pattern at all. In both A=37 and 39 cases, the measured values for this ratio are very similiar, at around 0.2. Thus any evidence for extra-nuclear effects in low-energy β and γ decays, as seen in investigations of ℓ-forbidden transitions, remains regrettably inconclusive.

REFERENCES

[1] E. Hagberg, T.K. Alexander, I. Neeson, V.T. Koslowsky, G.C. Ball, G.R. Dyck, J.S. Forster, J.C. Hardy, J.R. Leslie, H.-B. Mak, H. Schmeing and I.S. Towner, Nucl. Phys. **A571**, 555 (1994).

[2] E.G. Adelberger, J.L. Osborne, H.E. Swanson and B.A. Brown Nucl. Phys. **A417**, 269 (1984).

[3] T.K. Alexander, G.C. Ball, J.S. Forster, I.S. Towner, J.R. Leslie, H.-B. Mak, J.K. Johannson, J.A. Kuehner and J.C. Waddington, Nucl. Phys. **A526**, 407 (1991) and references therein.

[4] T.K. Alexander, G.C. Ball, J.S. Forster, I.S. Towner, J.R. Leslie and H.-B. Mak, Nucl. Phys. **A477**, 453 (1988).

[5] I.S. Towner, Phys. Rep. **155**, 263 (1987).

[6] I.S. Towner and F.C. Khanna, J. de Phys. **45**, C4-519 (1984).

[7] P.M. Endt, Nucl. Phys. **A521**, 1 (1990).

[8] Table of Isotopes, R.B. Firestone, ed. V.S. Shirley, John Wiley and Sons Inc., 1996.

[9] P.M. Endt and C. van der Leun, Nucl. Phys. **A310**, 1 (1978).

[10] P. Taras, A. Turcotte and R. Vaillancourt, Can. J. Phys. **50**, 1182 (1972).

[11] G. Azuelos and J.E. Kitching, Phys. Rev. **C15**, 1847 (1977).

[12] R.W. Kavanagh and D.R. Goosman, Phys. Lett. **12**, 229 (1964).

[13] F.M. Mann, H.S. Wilson and R.W. Kavanagh, Nucl. Phys. **A258**, 341 (1976).

[14] B.H. Wildenthal, Prog. in Part. and Nucl. Phys. **11**, ed. D. H. Wilkinson (Pergamon Press, Oxford, 1984) p. 5.

[15] W. Chung, Ph.D. thesis, Michigan State University, 1976; B.H. Wildenthal and W. Chung, in *Mesons in Nuclei*, edited by M. Rho and D.H. Wilkinson (North-Holland, Amsterdam, 1979), Vol.II.

[16] B.A. Brown, Phys. Rev. Lett. **69**, 1034 (1992)

[17] B.A. Brown and B.H. Wildenthal, Phys. Rev. **C28**, 2397 (1983)

[18] M.C. Etchegoyen, A. Etchegoyen, B.H. Wildenthal, B.A. Brown and J. Keinonen, Phys. Rev. **C38**, 1382 (1988)

[19] B.A. Brown and B.H. Wildenthal, At. Data Nucl. Data Tables **33**, 347 (1985)

[20] I.S. Towner and F.C. Khanna, Nucl. Phys. **A399**, 334 (1983); I.S. Towner and F.C. Khanna, Phys. Rev. Lett. **42**, 51 (1979).

[21] A. Arima, K. Shimizu, W. Bentz and H. Hyuga, Adv. in Nucl. Phys. **18**, 1 (1987)

[22] D.M. Brink and G.R. Satchler, *Angular Momentum* (Clarendon, Oxford, 1968)

[23] T.K. Alexander, B. Castel and I.S. Towner, Nucl. Phys. **A445**, 334 (1985).

[24] K. Kubodera, J. Delorme and M. Rho, Phys. Rev. Lett. **40**, 755 (1978).

[25] E.K. Warburton, J.A. Becker, B.A. Brown and D.J. Millener, Ann. Phys. **187**, 471 (1988).

[26] O. Häusser, Nucl. Phys. **A585**, 133c (1995)

[27] E. Hagberg, J.C. Hardy, V.T. Koslowsky and G. Savard, to be published.

TABLES

TABLE I. Gamma rays from the decay of ^{37}K.

E_γ (keV)	I_γ (rel) (%)	I_γ (abs) (ppm)[c]
879[a]		2[a]
1184.84(10)[b]	1.286(54)	263(14)
1386.25(13)[b]	0.211(14)	43(3)
1409.78(11)[b]	0.471(22)	96(6)
1611.24(10)[b]	1.417(58)	289(15)
2191.5(8)[b]	0.044(15)	9(3)
2490.0(3)[b]	0.13(2)	27(4)
2528[a]		1.8[a]
2795.97(15)	100	2.04(11)%
3169.65(30)[b]	0.13(1)	27(2)
3601.6(4)	1.052(44)	215(11)
3937.7(5)[b]	0.048(6)	9.7(12)

[a]inferred from in-beam experiments. See text.
[b]first observation
[c]result in parts per million, except where noted otherwise

TABLE II. Levels in ^{37}Ar populated in the decay of ^{37}K.

Present Expt.	Literature[a]		Beta feeding	
E_x (keV)	E_x (keV)	J^π	(ppm)[b]	log ft
0.00		$3/2^+$	97.89(11)%	3.66
1409.82(9)	1409.82(10)	$1/2^+$	42.2(75)	7.39
1611.26(8)	1611.27(7)	$7/2^-$	25(20)	7.51
2490.06(30)	2490.60(30)	$3/2^-$	29(4)	6.88
2796.11(10)	2796.10(30)	$5/2^+$	2.07(11)%	3.79
3169.80(30)	3171.30(140)	$5/2^+$	27(2)	6.35
3601.67(37)	3602.00(70)	$3/2^+$	224(12)	4.96
3937.95(50)	3936.70(40)	$3/2^+$	11.6(13)	5.78

[a]Ref. [7]
[b]result in parts per million, except where noted otherwise

TABLE III. Gamma-ray branching ratios of ^{37}Ar levels (%).

	E_{xf} (keV)			
E_{xi} (keV)	0	1410	1611	2217
2796	98.25(6)	0.214(9)	1.267(51)	<0.2
3602	96.0(14)	4.0(14)	<1.7	<11

TABLE IV. Effective coupling constants for the M1 and GT operators for mass, A=37, from the calculations of Towner and the data fits of Brown and Wildenthal.

	Towner[a]			Brown-Wildenthal[b]		
Notation[c]	IS	IV	GT	IS	IV	GT
$\delta g_{\rm S}(d\text{-}d)$	−0.147	−0.612	−0.240	−0.134	−0.830	−0.342
$\delta g_{\rm S}(s\text{-}s)$	−0.145	−0.633	−0.250	−0.054	−0.726	−0.312
$\delta g_{\rm L}(d\text{-}d)$	0.010	0.078	0.009	0.021	0.140	0.010
$\delta g_{\rm P}(d\text{-}d)$	−0.024	0.728	0.100	0.165	2.340	0.115
$\delta g_{\rm P}(d\text{-}s)$	−0.033	0.502	0.162	0.165	2.340	0.115

[a]Results from Ref. [5], but with two changes: first, the isobar coupling constant is reduced from the Chew-Low value to the quark-model value; second, the results for mass, A=37, are interpolated between values quoted for A=17 and A=39.

[b]From Ref. [17], the "A=18-38" fit for isoscalar (IS) electromagnetic operators; From Ref. [18], table I, column 4, for isovector (IV) electromagnetic operators; From Ref. [19], for Gamow-Teller (GT) operators.

[c]The argument in the effective coupling constants indicates the orbitals for which the value is operative. For the Gamow-Teller operator the results tabulated are for $\delta g_{\rm A}$, $\delta g_{\rm LA}$ and $\delta g_{\rm PA}$.

TABLE V. $B(GT)$ values for various states in ^{37}Ar fed by allowed transitions in the beta decay of ^{37}K.

		Theory[a]		
Transition	Experiment	T(USD)	T(CW)	BW(USD)
$B(GT; 3/2^+ \rightarrow 3/2_1^+)$	$3.38(8) \times 10^{-1}$	4.12×10^{-1}	4.81×10^{-1}	3.38×10^{-1}
$B(GT; 3/2^+ \rightarrow 1/2_1^+)$	$2.5(5) \times 10^{-4}$	0.5×10^{-4}	3.1×10^{-4}	0.1×10^{-4}
$B(GT; 3/2^+ \rightarrow 5/2_1^+)$	$1.0(5) \times 10^{0}$	1.1×10^{0}	1.1×10^{0}	0.9×10^{0}
$B(GT; 3/2^+ \rightarrow 5/2_2^+)$	$2.8(2) \times 10^{-3}$	6.1×10^{-2}	5.0×10^{-1}	5.0×10^{-2}
$B(GT; 3/2^+ \rightarrow 3/2_2^+)$	$6.4(4) \times 10^{-2}$	4.4×10^{-2}	1.1×10^{-1}	3.7×10^{-2}
$B(GT; 3/2^+ \rightarrow 3/2_3^+)$	$1.0(1) \times 10^{-2}$	7.9×10^{-2}	3.7×10^{-2}	6.7×10^{-2}

[a] *s-d* shell wavefunctions from the universal *s-d* interaction (USD), or the Chung-Wildenthal interaction (CW); and effective coupling constants from Towner (T) or Brown-Wildenthal (BW) as given in Table IV.

TABLE VI. Electromagnetic and weak rates (in nuclear magneton units) for the ℓ-forbidden transition $3/2^+ \rightarrow 1/2^+$ in A=37 nuclei.

		Theory[a]		
	Experiment	T(USD)	T(CW)	BW(USD)
$B(M1;^{37}\mathrm{K})$	$> 4.7 \times 10^{-3}$	9.1×10^{-3}	6.0×10^{-3}	1.6×10^{-4}
$B(M1;^{37}\mathrm{Ar})$	$7.1(23) \times 10^{-3}$	1.0×10^{-2}	6.2×10^{-3}	1.3×10^{-3}
$\mid M^{(0)} \mid$	$< 0.8 \times 10^{-2}$	2.2×10^{-3}	8.1×10^{-4}	1.2×10^{-4}
$\mid M^{(1)} \mid$	$> 7.6 \times 10^{-2}$	9.8×10^{-2}	7.8×10^{-2}	2.5×10^{-2}
$\mid M(GT) \mid$	1.6×10^{-2}	6.9×10^{-3}	1.8×10^{-2}	3.0×10^{-3}
$M(GT)/M^{(1)}$	< 0.2	0.07	0.22	0.12

[a] See corresponding footnote in Table V.

TABLE VII. First-forbidden $3/2^+ \rightarrow 3/2^-$ β transitions in ^{37}K and ^{39}Ca.

		Branch	
Parent	Final $3/2^-$ state (keV)	Experiment (ppm)	Predicted [25] (ppm)
^{37}K	2490	29(4)	250
^{39}Ca	3019	<3.3	51

FIGURES

FIG. 1. Schematic layout of the experimental setup. When the transport tape is moved the gas jet shutter blocks the He-jet nozzle (dotted position) and the accelerator beam is blocked as well. The scale is appropriate for all items shown except the concrete wall.

FIG. 2. Gamma-ray spectrum obtained from all samples. Each sample is counted for 3 seconds but this spectrum only shows those decays that occurred during the first 1.2 seconds. The symbols above the γ-ray peaks identify the activity and are explained in the box in the upper panel. The symbol S, SE and DE are used for peaks produced by coincident summing, single escape and double escape events, respectively. The 2796 and 3602 keV γ rays were previously known to originate from the decay of ^{37}K; eight new γ rays were found in this experiment.

FIG. 3. Gamma-ray spectra from the full three-second decay observation of all samples. *a)* Expanded region around the 1386 and 1410 γ-ray peaks. These two γ-ray transitions feed and de-populate the $1/2^+$, 1410 keV state, respectively. The beta side-feeding to this state is ℓ-forbidden. The 1460 keV γ-ray peak from ^{40}K room background is present as a result of random scintillator coincidences. Each channel is 1 keV wide. *b)* Expanded region around two γ-ray peaks from ^{37}K that are barely visible in Fig. 2. Each channel is 2 keV wide.

FIG. 4. Proposed decay scheme for ^{37}K. The numbers above each γ-ray transition are energies in keV and the absolute intensities per ^{37}K decay in ppm, unless otherwise indicated. The beta branching ratio is also given in ppm, unless otherwise indicated.

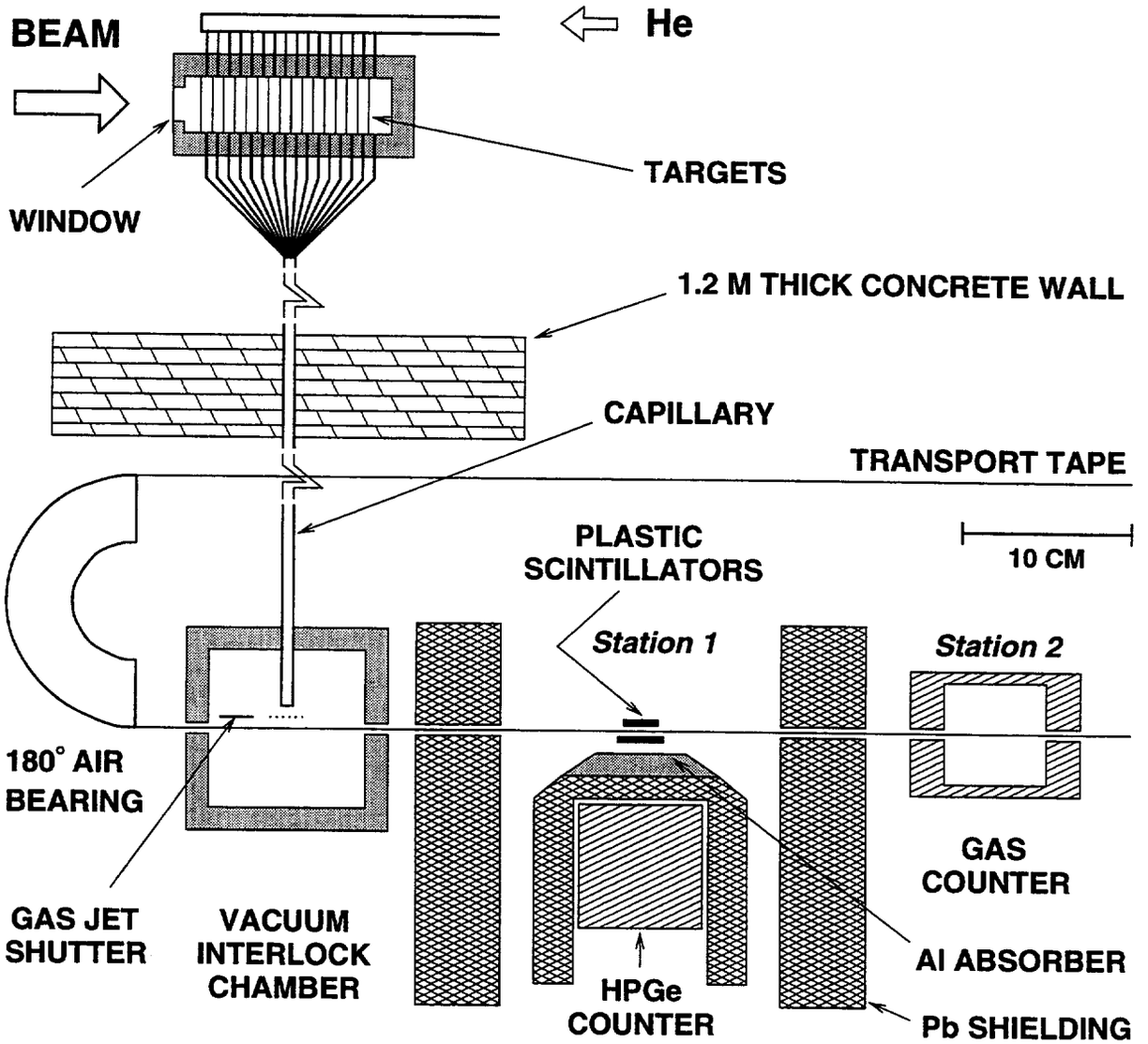
BEAM
He
WINDOW
TARGETS
1.2 M THICK CONCRETE WALL
CAPILLARY
TRANSPORT TAPE
PLASTIC
SCINTILLATORS
10 CM
Station 1
Station 2
180° AIR
BEARING
GAS JET
SHUTTER
VACUUM
INTERLOCK
CHAMBER
GAS
COUNTER
Al ABSORBER
HPGe
COUNTER
Pb SHIELDING

Fig 1

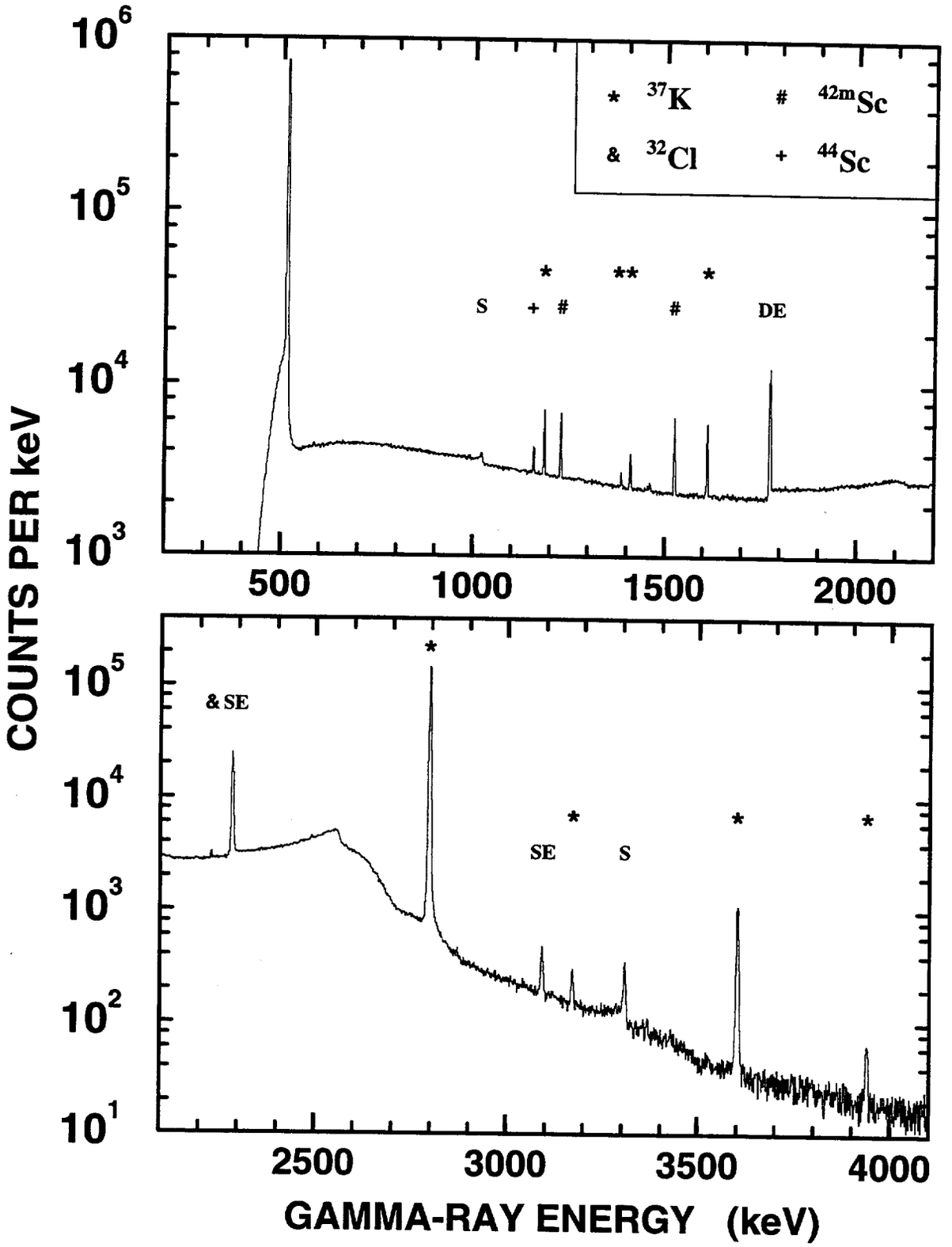
* ^{37}K
# ^{42m}Sc
& ^{32}Cl
+ ^{44}Sc
S
DE
& SE
SE
S
COUNTS PER keV
GAMMA-RAY ENERGY (keV)

Fig 2

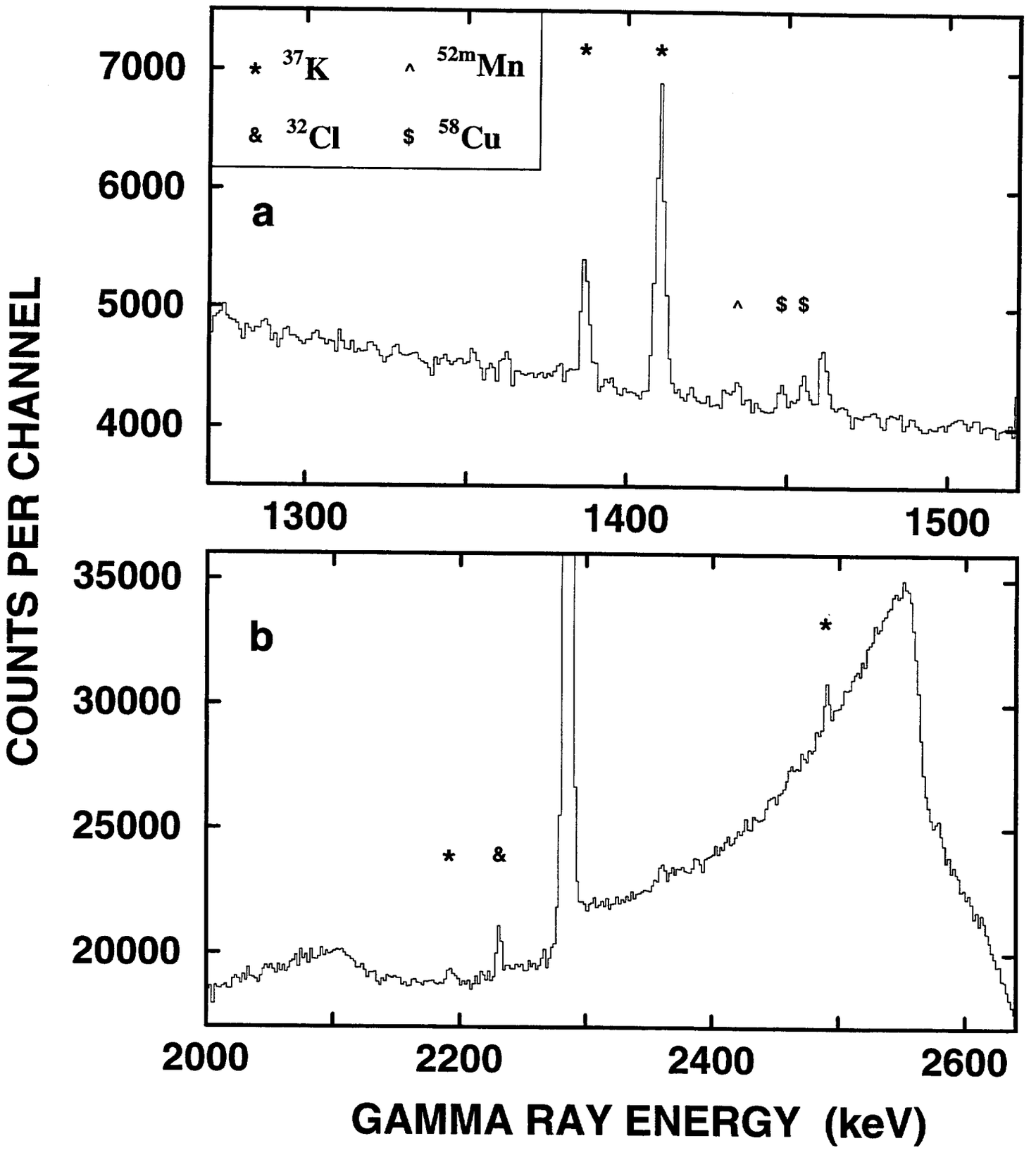
* ^{37}K
^ ^{52m}Mn
& ^{32}Cl
$ ^{58}Cu
a
b
7000
6000
5000
4000
1300
1400
1500
35000
30000
25000
20000
2000
2200
2400
2600
COUNTS PER CHANNEL
GAMMA RAY ENERGY (keV)

Fig 3

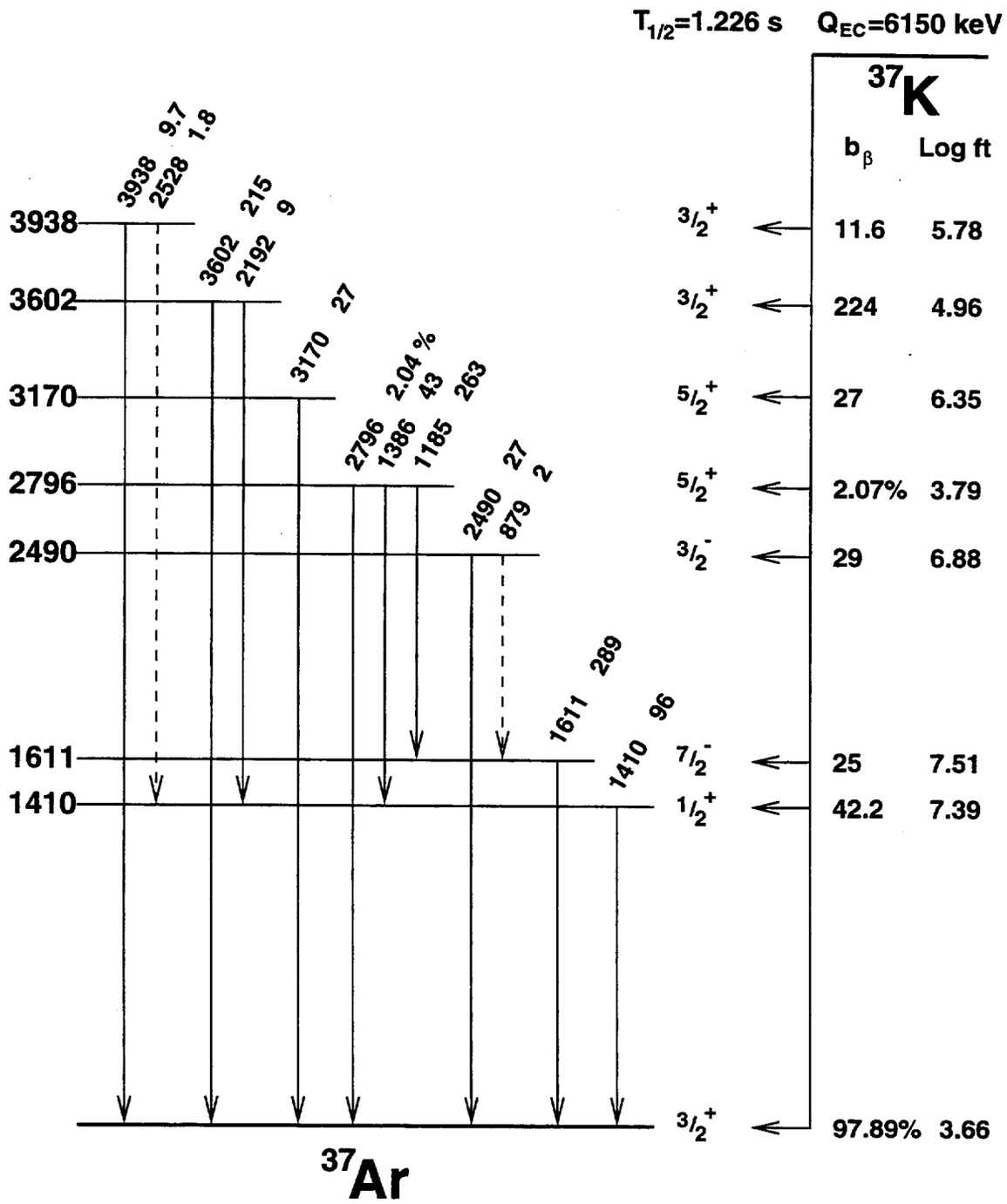
T1/2=1.226 s
QEC=6150 keV
37K
bβ
Log ft
3938
3602
3170
2796
2490
1611
1410
3/2+
11.6
5.78
3/2+
224
4.96
5/2+
27
6.35
5/2+
2.07%
3.79
3/2-
29
6.88
7/2-
25
7.51
1/2+
42.2
7.39
3/2+
97.89%
3.66
37Ar

Fig 4